Novel Concentric Hexagonal-Shaped RFID Tag Antenna with T-Shaped Stub Matching

Mohammad Alibakhshikenari, *Member, IEEE*, Bal S. Virdee, *Senior Member, IEEE*, Ayman A. Althuwayb, Kai-Da Xu, *Senior Member, IEEE*, Chan Hwang See, *Senior Member, IEEE*, Salahuddin Khan, Ikmo Park, *Senior Member, IEEE*, Francisco Falcone, *Senior Member, IEEE*, Ernesto Limiti, *Senior Member, IEEE*

***Abstract*— This paper presents a unique concentric hexagonal-shaped ring antenna for radio frequency identification (RFID) tags. The rings are excited with a common microstrip feedline. The radiation characteristics of the antenna is improved by locating a horizontal a parasitic element in the vicinity of the hexagonal-shaped rings. The proposed antenna was used in the implementation of a 3×1 antenna array. The impedance match of the 3×1 RFID tag was enhanced by incorporating a T-shaped stub. The antenna is designed to operate at the UHF band from 800 MHz to 960 MHz. It was implemented on FR-4 substrate with dielectric constant and thickness of 4.3 and 1.6 mm, respectively. The size of the RFID tag antenna is 36×10 mm^2. Its impedance was matched to Alien Higgs RFIC chip of impedance 10 – j 82.5 Ω at 895 MHz. Measured results show the proposed RFID tag antenna provides an impedance bandwidth, maximum gain and radiation efficiency of 160 MHz, 2 dBi, and 66.5%, respectively. With effective isotropic radiated power (EIRP) limited to 36 dBm to comply with FCC regulations for UHF band RFIDs it radiates in the broadside direction over a range of 9 m making it desirable for various applications including supply chain management, logistic control, and vehicle identification.**

***Index Terms*— RFID tag, concentric hexagonal-shaped ring antenna, microstrip integrated circuits, UHF band, impedance matching circuit, effective isotropic radiated power (EIRP).**

I. INTRODUCTION

Radio Frequency Identification (RFID) has become an indispensable technology for automatic contactless identification of objects of interest. RFIDs are used for numerous applications such as stock management in retail stores, tracking of goods in logistics supply chains, controlling access to buildings, airport security with E-passport, electronic toll payment for vehicles, ignition keys for anti-theft feature in high end cars, livestock identification and management in farms, etc. [1]. The frequency bands assigned for RFID applications include LF (125–134 kHz), HF (13.56 MHz), UHF (840–960 MHz), and microwave (2.45 and 5.8 GHz). Among these frequency bands, UHF RFID systems are more attractive than others due to fast data transfer speed, greater storage capability and higher reading range. Each country has allocated a specific frequency band within 840–960 MHz for UHF RFID system, e.g., India (865–867 MHz), Australia (920–926 MHz), Taiwan (920–928 MHz), Japan (952–956 MHz), North America (902–928 MHz), Korea (908.5–910 MHz), Europe (865–868 MHz), China (920.5–924.5 MHz), Singapore (866–869 MHz and 923–925 MHz), etc. [2].

An RFID system consists of a tag and a reader, where the reader transmits an interrogating radio frequency (RF) signal to the tag. The RF signal is converted to DC voltage by the passive tag to electrically power it. The tag then sends a reply signal to the reader to complete the communication. A passive RFID tag is composed of an application specific integrated circuit (ASIC) and an antenna. RFID systems are designed to operate at either the near-field or far-field mode. RFID systems operating in the low frequency (LF) and high frequency (HF) bands work using near-field electromagnetic coupling with load modulation principle [3], and RFID systems in the UHF band operate in the far-field using backscattered modulation [4]. For near-field coupling, both reader and tag use coil-based antennas with power coupling between them based on transformer principle. In far-field communication, the reader sends a modulated signal with unmodulated carrier pulses, which is used to energize the passive tag. When these unmodulated carrier pulses are converted to DC voltage by the tag, a potential difference is developed across its terminals to power the chip in the tag. The tag consequently replies to the reader via its antenna by

This project has received funding from Universidad Carlos III de Madrid and the European Union's Horizon 2020 research and innovation program under the Marie Sklodowska-Curie Grant 801538. Also, this work is partially supported by RTI2018-095499-B-C31, Funded by Ministerio de Ciencia,Innovación y Universidades, Gobierno de España (MCIU/AEI/FEDER,UE). Additionally, it received funding from the Researchers Supporting Project number (RSP-2021/58), King Saud University, Riyadh, Saudi Arabia.

M. Alibakhshikenari is with the Department of Signal Theory and Communications, Universidad Carlos III de Madrid, 28911 Leganés, Madrid, Spain (mohammad.alibakhshikenari@uc3m.es).

B. S. Virdee is with the London Metropolitan University, Center for Communications Technology, London N7 8DB, U.K. (e-mail: b.virdee@londonmet.ac.uk).

A. A. Althuwayb is with the Electrical Engineering Department, Jouf University, Sakaka, Aljouf 72388, Saudi Arabia (e-mail: aaalthuwayb@ju.edu.sa).

K. D. Xu is with the School of Information and Communications Engineering, Xi'an Jiaotong University, Xi'an 710049, China (e-mail: kaidaxu@ieee.org).

C. H. See is with the School of Engineering and the Built Environment, Edinburgh Napier University, 10 Colinton Rd., Edinburgh, EH10 5DT, U.K. (e-mail: c.see@napier.ac.uk)

S. Khan is with College of Engineering, King Saud University, Riyadh, Saudi Arabia (e-mail: drskhan@ksu.edu.sa).

I. Park is with the Department of Electrical and Computer Engineering, Ajou University, 206 Worldcup-ro, Youngtong-gu, Suwon 16499, Republic of Korea (e-mail: ipark@ajou.ac.kr).

F. Falcone is with the Electric, Electronic and Communication Engineering Department, Public University of Navarre and also with the Institute of Smart Cities, Public University of Navarre, 31006 Pamplona, Spain (e-mail: francisco.falcone@unavarra.es)

E. Limiti is with the Electronic Engineering Department, University of Rome "Tor Vergata", Via del Politecnico 1, 00133 Rome, Italy (e-mail: limiti@ing.uniroma2.it).

switching its input impedance between two states. One of them is the match state when the chip impedance is fully matched with the tag antenna. In this state, the chip is powered up. In the other state a strong mismatch results in backscattering modulation. Thus, the tag antenna is a crucial element because the overall performance of RFID system depends on the performance of the tag.

Numerous RFID tag antenna structures have been reported recently. For example, a planar inverted-F antenna in [5] uses two orthogonally directed electric currents to achieve a quasi-isotropic radiation pattern. An ultra-high-frequency (UHF) band RFID antenna in [6] is spiral shaped meander line with loading. This antenna was optimized using the guided artificial bee colony (GABC) algorithm. In [7], a fork-shaped tag antenna with two parasitic patches is presented. The parasitic patches are also used to control the input impedance of the antenna. In [8] a CPW-fed folded-slot monopole antenna is reported for active RFID tags at 5.8 GHz. Reported in [9,10] are crossed-dipole circularly polarized antennas with a modified *T*-match network. The overall size of this antenna is larger than that for a linearly polarized antenna at the same operating frequency. In [11], a single sided dual antenna with an electromagnetic bandgap structure is proposed to enhance the gain. This antenna is made of two radiating elements, one of which is for receiving the signal and the other for backscattering. A dual-band antenna for high-frequency band and ultra-high frequency band RFID systems based on the Hilbert-curve fractal is described in [12]. A hollowed-out meander dipole antenna for printed RFID tags is developed in [13] to reduce conductive ink. In [14] dual band functionality for Europe (867 MHz) and Japan (956 MHz) UHF RFID is obtained by using impedance perturbation method in a folded dipole antenna. A two quarter-wave patch tag antenna with loop feed is presented in [15], in which low-cost feed loop and radiating antennas were designed separately.

More recently, the state-of-the-art RFID antennas include a near-field RFID tag designed to operate at 900 MHz [16]. This antenna consists of quadruple fan-shaped small loops and the middle feeding lines of each loop located at the top and bottom of the substrate are excited using vias. The range of this antenna is limited to 50 mm. In [17] the UHF RFID tag is based on a circularly polarized (CP) patch antenna. Miniaturization of the antenna was achieved by applying a combination of cross-shaped and L-shaped slots in the radiator. In conjunction, the right-hand circular polarization was achieved by asymmetrically truncating all four corners of the square-shaped radiator. The read range of the tag is 5.8 m however its gain is -7.1 dBi. In [18] the RFID tag is based on a cylindrical ceramic resonator that supports a localized magnetic mode. A miniature non-resonant metal split ring with a standard RFID chip soldered in the ring's gap is placed on top of the dielectric cylinder. Near-field coupling converts the displacement currents of the resonator into conduction current flow in the ring that energizes the operation of the chip. The read range of the tag is 5 m. The RFID antenna in [19] comprises a radiating patch with double I-shaped slots and a ground layer that is shorted to a narrow inductive plate. Loading a closed slot in the center of the patch and the open slits enables flexible frequency tuning to match the complex impedance of the microchip used. The antenna has a gain of -2.3 dBi and a range of 8.1 m.

The design and fabrication of the above antennas is considered generally complex and therefore not cost-effective. Moreover, the antennas have a narrow frequency bandwidth, low gain performance and relatively small read range. In this paper to address these shortcomings a novel UHF RFID tag antenna is proposed comprising 3×1 linear array of concentric hexagonal-shaped ring radiators. The three antenna elements are symmetrical about the origin and have a common microstrip feedline. The impedance matching between the antennas is achieved by (i) inserting a *T*-shaped stub on the feedline between the antennas, and (ii) by inductively coupling the antennas to a horizontal parasitic element located in the vicinity of the 3×1 array. The antenna was analyzed and optimized using CST-Microwave Studio which is a powerful and highly accurate 3D electromagnetic tool.

The paper is organized as follow: section II describes the design of the RFID tag antenna, in section III the antenna is compared with other RFID tag antennas published to date, and the paper is concluded in section IV.

II. RFID-Tag Antenna Design

Meander-line antennas are popular among various tag antennas due to their simple structure and omnidirectional radiation pattern. However, these types of antennas have disadvantages of low radiation efficiency because of two factors, i.e., the currents in the adjacent sides of the meander line are in opposite directions resulting in partial cancellation of the fields when the spacing between the bends is too close; and secondly, the line width of the meander-line is typically made to realize a large bandwidth however this is not consistent to match the antenna with the impedance of free-space.

A. The Proposed RFID Tag Antenna Geometry

To overcome the issues with meander-line antennas proposed here is an innovative antenna for RFID tags, which is shown in Fig.1(a). The antenna consists of three elements, namely, concentric hexagonal-shaped rings, a common microstrip feedline that is connected to the hexagonal rings, and a horizontal parasitic microstrip-line that is inductively coupled to the hexagonal-shaped rings. The length of the parasitic element contributes towards improving the impedance matching with the load, which is an Alien Higgs tag chip. The magnitude of mutual coupling between the parasitic element and antenna is governed by their proximity.

The hexagonal rings constituting the antenna function as individual resonating structures whose frequency is determined by the length of their circumference, which is defined approximately by $f_o = c/2\pi R\sqrt{\varepsilon_{eff}}$, where c is speed of light, ε_{eff} is effective permittivity of the substrate, and R is radius of the ring. The number of rings control the bandwidth of the antenna.

The antenna was constructed on FR4 substrate with dielectric constant of ε_r=4.3, tanδ = 0.025, and thickness of 1.6 mm. The dimensions of the antenna have been optimized using CST-Microwave Studio to operate over 883 MHz to 888 MHz with a peak resonance frequency centered at 886 MHz. The antenna is designed for use with the Alien Higgs tag chip. The

impedance of the chip is frequency dependent, and at 886 MHz it is 10 – j 82.5 Ω.

The reflection-coefficient frequency response of the proposed reference antenna with and without the horizontal parasitic microstrip-line is shown in Fig.1(b). It is evident from this response that with the parasitic line the reflection-coefficient is improved. Line width of 0.25 mm provided the optimum reflection-coefficient. In this case the antenna exhibits a limited bandwidth of 2.83 MHz for $|S_{11}| \leq$-10 dB between 883 MHz to 885.8 MHz. Over this frequency range the corresponding antenna gain and radiation efficiency performance shown in Fig.2 vary between -1.05 dBi and -1 dBi, and 21.6% and 22.4%, respectively.

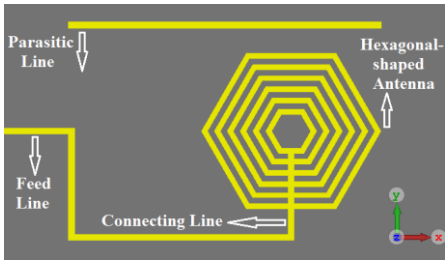

(a)

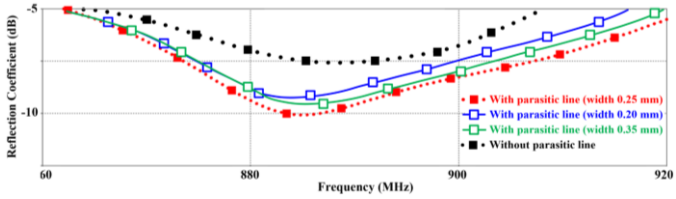

(b)

Fig.1. The proposed reference antenna for RFID tags, (a) layout circuit, and (b) reflection-coefficient frequency response.

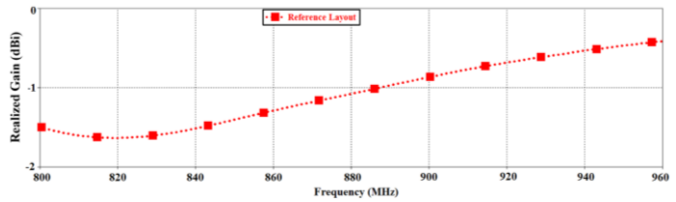

(a)

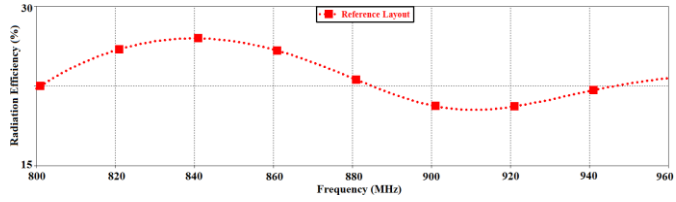

(b)

Fig.2. Radiation properties of the proposed reference RFID tag antenna as a function of frequency, (a) antenna gain, and (b) radiation efficiency.

B. The Proposed RFID Tag Antenna with Increased Aperture

To improve the performance of the proposed antenna its effective aperture is increased by adding in series an identical antenna, as shown in Fig.3(a). The antennas are serially fed, and the length of the connecting microstrip-line is made such that there is phase coherence in the current at the input of the radiators, which is important to realize optimum radiation characteristics. The parasitic element above the antenna is extended to cover the two radiators. The performance of the antenna when it's excited from the left-hand side are shown in Fig.3(b)-(d). The impedance bandwidth of the antenna for $|S_{11}| \leq$-10 dB is 37 MHz from 867 MHz to 904 MHz. The corresponding antenna gain and radiation efficiency over this frequency range varies between -0.8 dBi and -0.41 dBi, and 35.5% and 37.7%, respectively. Compared to the single antenna scenario this constitutes an average improvement in gain and efficiency of 0.56 dBi and 15.2%, respectively.

C. Extended Aperture RFID Tag Antenna Loaded with IMC

To counteract the highly capacitive impedance of the RFID chip the impedance of the antenna needs to be highly inductive to optimize power transfer between them. Hence, an impedance matching circuit (IMC) is necessary to conjugately match the impedances of the chip and the antenna. This was achieved by incorporating at the mid-point of the interconnecting microstrip-line a *T*-shaped stub, as shown in Fig.4. The inductance of antenna can be altered by simply varying the dimensions of the stub. It is shown that after applying the IMC the impedance bandwidth and impedance match of the antenna is significantly improved. This is achieved without increasing the antenna dimensions. The impedance match for $|S_{11}| \leq$-10 dB now extends from 833 MHz to 914 MHz. The corresponding gain and efficiency now vary between -1.08 dBi to 0.48 dBi, and from 48.5% to 57.2%, respectively. The bandwidth is improved by 44 MHz, and the improvement in the average gain and efficiency are 0.3 dBi and 16.2%, respectfully.

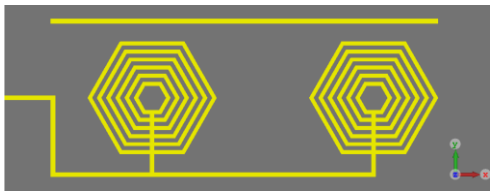

(a)

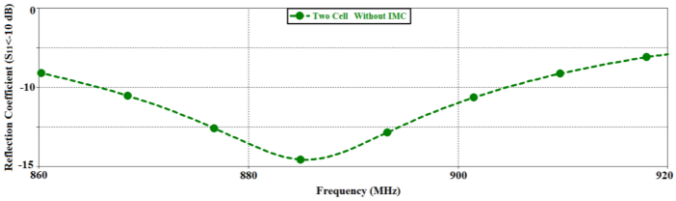

(b)

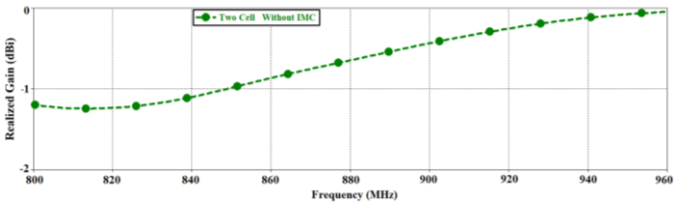

(c)

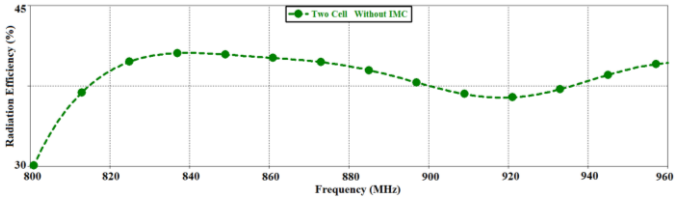

(d)

Fig.3. RFID tag antenna using two identical and serially fed radiating elements, (a) layout, (b) reflection-coefficient as a function of frequency, (c) antenna gain as a function of frequency, and (d) radiation efficiency as a function of frequency.

D. Optimized IMC Loaded RFID Tag Antenna

The radiation elements of the proposed antenna were increased from two to three. This was done to investigate the degree of improvement in the antenna's performance. Fig.5 shows the layout and the fabricated three-element antenna. The radiation characteristic of the antenna is determined by the current distribution on the radiating elements constituting the array. It is therefore important to ensure the physical length of the interconnecting feedlines are such that the current is in phase at the input of the radiation elements.

The optimized values of proposed antenna parameters are given in Table I. Fig. 5(d)-(f) show the reflection-coefficient, antenna gain and radiation efficiency of the three-element antenna in relation to the reference and two-element antennas. It is observed that the inclusion of the *T*-matching stubs in the array effects the array's directivity that causes the inconsistent differences in the gain and efficiency response over the 880 MHz – 900 MHz frequency band. The gain and efficiency vary between 1.7 dBi to 2 dBi, and 56.8% to 66.5%, respectively. Compared with the two-element antenna with IMC the three-element exhibits an average improvement in gain and efficiency of 2.05 dBi and 8.65%, respectively. The improvement in the impedance bandwidth is 79 MHz, which is an improvement of 97.5%. The performance of the antenna is summarized in Table II.

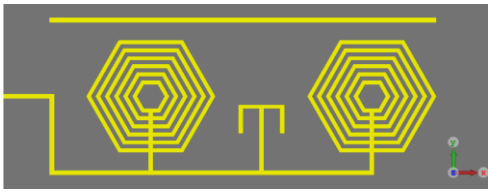

(a)

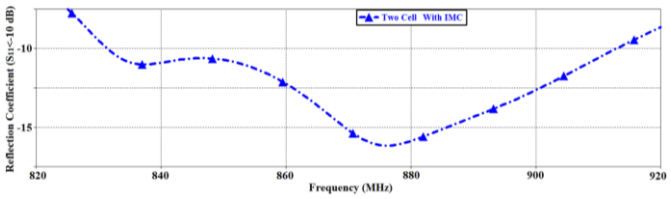

(b)

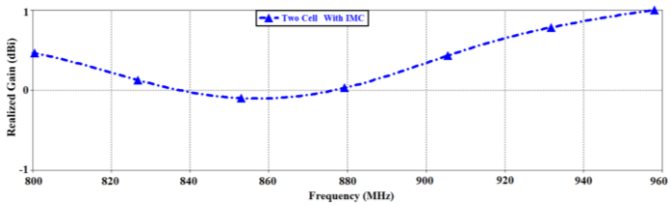

(c)

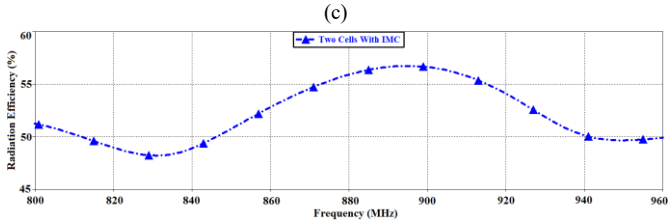

(d)

Fig.4. Two radiating element RFID tag loaded with internal impedance matching element consisting of a *T*-shaped stub, (a) layout circuit, (b) reflection-coefficient as a function of frequency, (c) antenna gain as a function of frequency, and (d) radiation efficiency as a function of frequency.

The equivalent electrical circuit model of the proposed three-element antenna with the *T*-matching network is shown in Fig.6. The circuit consists of three resonance elements made of the hexagonal-shaped rings that are interconnected via two *T*-shaped stubs. The individual antennas are inductively coupled to the horizontal common parasitic element and excited by a common feedline. By modifying the length and width of the *T*-shaped stub, the inductance of antenna can be varied without changing other antenna parameters.

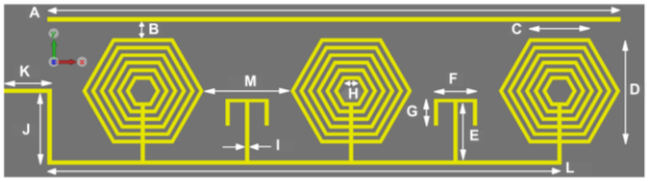

(a)

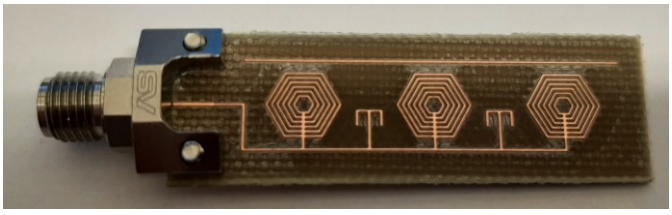

(b)

(c)

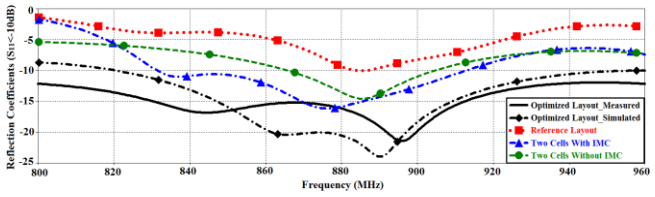

(d)

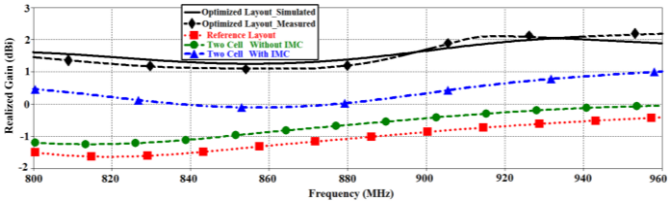

(e)

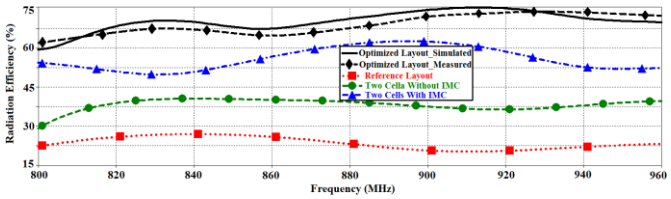

(f)

Fig.5. Optimized three-element RFID tag antenna, (a) layout circuit, (b) fabricated prototype (top-side), (c) fabricated prototype (bottom-side), (d) reflection-coefficient as a function of frequency, (e) antenna gain as a function of frequency, and (f) radiation efficiency as a function of frequency.

TABLE I
STRUCTURAL PARAMETERS OF THE PROPOSED UHF RFID-TAG THREE ELEMENT ANTENNA (Units in millimeters)

A	B	C	D	E	F	G
33	1	3.5	6	3.5	2.5	1.5

H	I	J	K	L	M	Overall dimensions
1.5	0.25	4.2	2.8	29.5	5	36×10×1.6

TABLE II
PERFORMANCE PARAMETERS

Parameters	Reference antenna	2-element antenna with IMC	3-element antenna with IMC (measured)
Impedance bandwidth (MHz)	883 – 885.8	833 – 914	800 – 960
Gain (dBi)	0 – -0.1	-1.08 – 0.48	1.7 – 2
Efficiency (%)	21.6 – 22.4	48.5 – 57.2	56.8 – 66.5

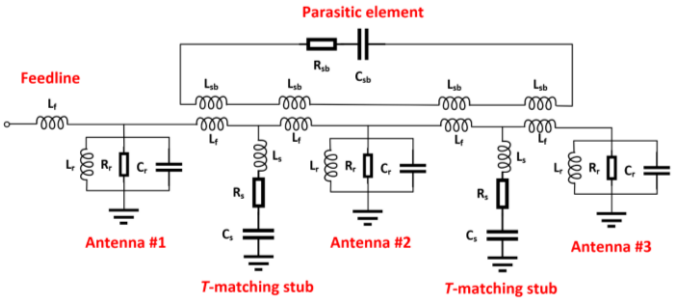

Fig.6. Equivalent *RLC* circuit model of the proposed three-element RFID tag antenna.

As stated earlier the RFID chip has a highly capacitive impedance. To counteract this capacitance the antenna's impedance needs to be conjugately match to the chip impedance. The real and imaginary parts of the input impedance of the antenna are shown in Fig. 7. The input impedance at 895 MHz is 10 + j82.5 Ω, which approximates to the complex conjugate of chip impedance.

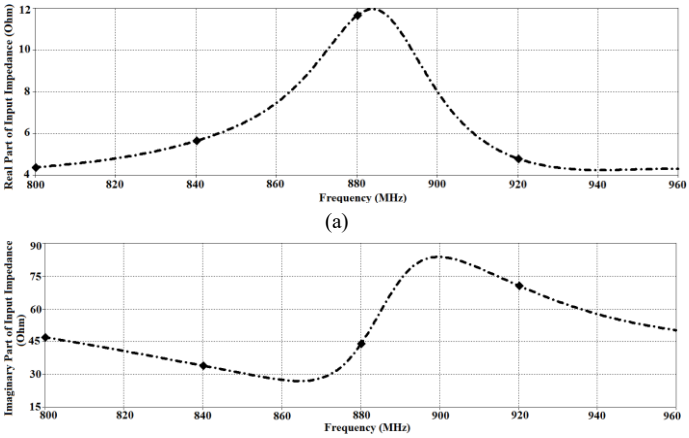

Fig.7. Input impedance of the proposed three-element RFID tag antenna as a function of frequency, (a) real part, and (b) imaginary part.

As mentioned earlier the radiation characteristics of the proposed antenna is determined by the current density distribution over it. The distance between the radiators in the 3×1 antenna array is made such that there is phase coherency at the input of each radiator in the array. This is an important condition to prevent the radiation pattern distorting. Surface current density distribution on the radiating three-element antenna at spot frequencies of 820 MHz, 890 MHz, and 960 MHz in Fig.8 shows the concentration of current is intense on the feedline, the *T*-shaped stubs and the input to the hexagonal-shaped multi ring antenna. The intensity of the current density is particularly strong at 890 MHz.

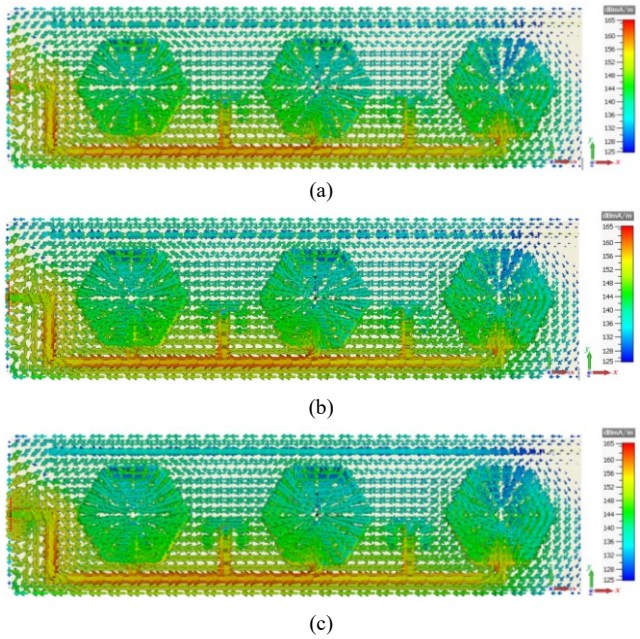

Fig.8. Surface current densities distributions over the proposed three-element RFID tag antenna at (a) 820 MHz, (b) 890 MHz, and (c) 960 MHz.

The simulated 3D radiation pattern at 895 MHz is shown in Fig.9(a). The corresponding measured radiation patterns in the orthogonal planes are shown in Fig.9(b). A standard measurement setup, shown in Fig. 10, was used to measure the antenna's radiation pattern. The floor of the anechoic chamber and the ceiling are lined with 900 mm long absorbers, other walls with 450 mm long RF absorbers. The wideband horn antenna on the right-hand side is fixed. The horn antenna is the measurement antenna. The antenna under test (AUT) is rotated about two axes, and its movements are computer controlled. The antenna radiates in the broadside in the *E*-plane and approximately omnidirectionally in the *H*-plane. The radiation in backside is attenuated by 30 dB.

The main parameter that is used to define an RFID tag is its read range. This is the maximum distance at which the RFID reader can detect the backscattered signal from the tag. The read range is determined by the antenna gain, its orientation, and the conditions of the environment. The maximum read range R_m can be calculated using [20]

$$R_m = \frac{\lambda}{4\pi}\sqrt{\frac{P_t G_t G_r}{P_{th}}\left\{1-\left[\left|\frac{(Z_c-Z_a)}{(Z_c+Z_a)}\right|^2\right]\right\}} \qquad (1)$$

Where λ is the operating wavelength, P_t is the power radiated by the reader, and G_t is the gain of the transmitting antenna, G_r is the gain of receiving tag antenna, and P_{th} is the minimum power needed by the RFID tag chip.

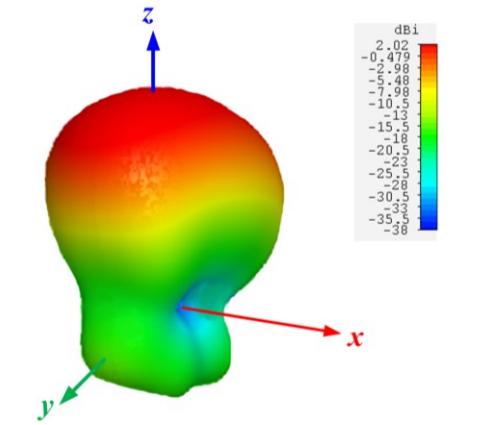

(a)

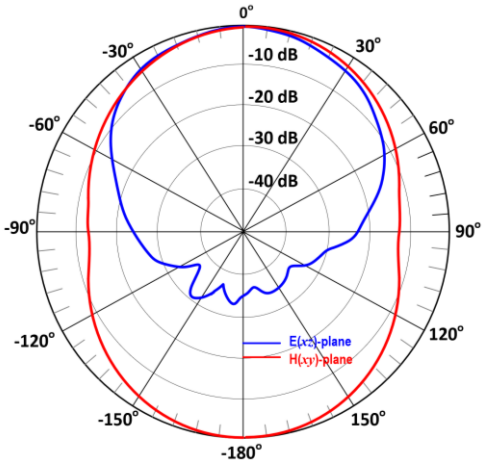

(b)

Fig.9. Far-field radiation patterns at 895 MHz, (a) simulated 3D radiation pattern, and (b) normalized measured *E*-plane (*xz*-plane) and *H*-plane (*xy*-plane).

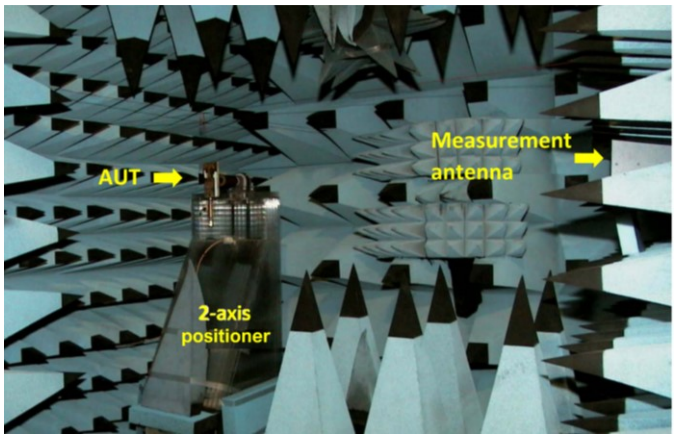

Fig.10. Antenna measurement setup.

The read distance of the RFID tag antenna was measured in an anechoic chamber in accordance with the EPCglobal static test standard [21]. The antenna tag was placed on a platform and facing the interrogator antenna. Rather than gradually positioning the RFID tag away from the interrogator antenna, a power attenuator was used to simulate the power loss caused by transmission distance.

The permissible value of the effective isotropic radiated power ($EIRP = P_t G_t$) in Europe is 3.3 W, whereas in American it is 4 W. The proposed antenna is designed for Alien Higgs IC chip with P_{th} = -12 dBm. The gain of the three-element antenna (G_r) is shown in Fig.5. The read range as a function of frequency for *EIRP* = 4 W using the proposed three-element antenna is shown in Fig.11. It is evident from the graph that with the proposed antenna a read range of 9 m can be achieved at 890 MHz.

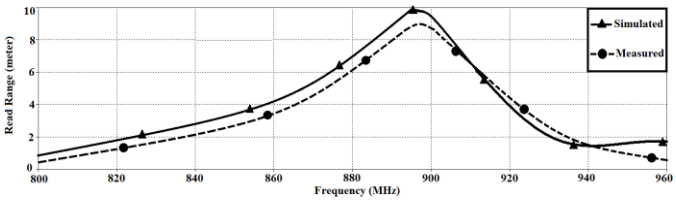

Fig.11. Simulated and measured read range of the proposed three-element RFID tag antenna.

III. Performance Comparison

The salient features of the proposed three-element RFID tag antenna are compared with other tag antennas reported to date in Table III. The proposed antenna is a unique design comprising 3×1 matrix of radiators. Another 2×2 RFID antenna array was recently reported in [17]. Compared with [17] the proposed antenna exhibits substantially greater bandwidth by a factor of 46.7, a gain higher by 9.1 dB, and a range which is 55% bigger. Compared with other cited references in the table the proposed antenna has significantly larger bandwidth and longer read range. The large bandwidth enables transmission of large amounts of data more reliably. The performance of the proposed RFID tag antenna is better than prior art because it includes *T*-matching stubs inserted between the hexagonal-shaped ring radiators, and secondly the distance between the radiators in the proposed array is such that the phase is coherent at the input of each radiator.

VI. Conclusion

A unique three-element antenna is shown to be effective for UHF-band RFID tag applications. The radiation elements comprise of concentric hexagonal-shaped rings that are excited with a common feedline. The antenna was conjugately impedance matched to an Alien Higgs RFIC chip. This was done by using *T*-matching networks located between the radiating elements. The overall size of the RFID tag antenna is 36×10 mm^2. Measurements show the proposed RFID tag antenna exhibits maximum gain of 2 dBi and maximum radiation efficiency of 66.5% over a frequency bandwidth of 160 MHz between 800 - 960 MHz. The large bandwidth makes it useful for high-capacity data applications. Moreover, the antenna radiates power over a long range of 9 m which makes it suitable for various application such as inventory tracking, access control, and theft deterrence in shops.

TABLE III
COMPARISON OF THE PROPOSED THREE-ELEMENT RFID-TAG ANTENNA WITH VARIOUS DESIGN APPROACHES.

Ref.	Substrate, Thickness	Size (mm^2)	Antenna geometry	-10 dB Bandwidth (MHz)	Max. Gain (dBi)	Max. Reading Range (m)
[16]	RF4, 0.8 mm	40 × 40	Quadruple loop	23	-	0.05
[17]	EPDM foam, 4.5 mm	50 × 50	2 × 2 array	3	-7.1	5.8
[18]	Ceramic, 20 mm	34 (diameter × 20	Ceramic disk	23	-	5.0
[19]	FR4, 0.8 mm & 0.2 mm	28 × 25	Patch with I-shaped slots	37	-2.3	8.1
[20]	FR4, 1.6 mm	50 × 12	Meander line dipole	14	-7.5	3.5
[22]	PET, 75 mm	89.2 × 29	Double UT	102	1.9	-
[23]	PET, 50 mm	79.3 × 53.1	Bend dipoles	78	-	2.4
[24]	FR4, 2 mm	96 × 50	Patch with pair of U slots	25	-	4.5
[25]	FR4, 2 mm	65 × 65	Patch with two slots	10	-	3.5
[26]	Foam & FR4, 4.6 mm	106 × 44	Double patch shorted to ground	70	-	6.2
[27]	RT5880, 1.58 mm	137 × 32	Two quarter patches shorted to ground	80	-	5.0
[28]	FR4, 3.2 mm	56 × 26	Dual-layer	20	-3.8	4.0
[29]	Paper, 0.5 mm	80 × 34	Dual-layer inverted-F antenna	40	1.8	5.8
[30]	Foam, 1.6 mm	23 × 16	Dipole patch split by meandered slot	-	-10.3	4.5
[31]	PET + Softlon, 1.6 mm	30 × 30	Orthogonal dipolar patches	100	-12.0	3.5
This work	**FR4, 1.6 mm**	**36 × 10**	**3 × 1 array**	**160**	**2.0**	**9.0**

PET stands for Polyethylene Terephthalate.
EPDM stands for Ethylene Propylene Diene Monomer.

REFERENCES

[1] Paret, D., RFID at Ultra and Super High Frequencies: Theory and Application, John Wiley & Sons, 2009.

[2] Finkenzeller, K., RFID Handbook: Radio-Frequency Identification Fundamentals and Applications, Wiley, New York, 2004.

[3] Heidrich, J., D. Brenk, J. Essel, G. Fischer, R. Weigel, E. Nuremberg, S. Schwarzer, and K. Seemann, "The roots, rules, and rise of RFID," IEEE Microwave Magazine, vol. 11, pp. 78–86, May 2010.

[4] Loo, C.-H., K. Elmahgoub, F. Yang, A. Elsherbeni, D. Kajfez, A. Kishk, and T. Elsherbeni, "Chip impedance matching for UHF RFID tag antenna design," Progress in Electromagnetics Research, vol. 81, pp. 359–370, 2008.

[5] Cho, C., H. Choo, and I. Park, "Printed symmetric inverted-F antenna with a quasi-isotropic radiation pattern," Microwave and Optical Technology Letters, vol. 50, pp.927–930, April 2008.

[6] Goudos, S. K., K. Siakavara, A. Theopoulos, E. E. Vatiadis, and J. N. Sahalos, "Application of Gbest guided artificial bee colony algorithm to passive UHF RFID tag design," International Journal of Microwave and Wireless Technologies, vol. 8, pp. 537–545, May 2016.

[7] Kim, K. H., J. G. Song, D. H. Kim, H. S. Hu, and J. H. Park, "Fork-shaped RFID tag antenna mountable on metallic surfaces," Electronics Letters, vol. 43, pp.1400–1402, December 2007.

[8] Bhaskar, S., S. Singhal, and A. K. Singh, "Folded-slot active tag antenna for 5.8 GHz RFID applications," Progress in Electromagnetics Research C, vol. pp.82, 89–97, March 2018.

[9] Bhaskar, S. and A. K. Singh, "Linearly tapered meander line cross dipole circularly polarized antenna for UHF RFID tag applications," International Journal of RF and Microwave Computer Aided Engineering, e21563, 2018.

[10] Tran, H. H., S. X. Ta, and I. Park, "A compact circularly polarized crossed-dipole antenna for an RFID tag," IEEE Antennas and Wireless Propagation Letter, vol. 14, pp.674–677, March 2015.

[11] Kamalvand, P., G. K. Pandey, and M. K. Meshram, "A single-sided meandered-dual-antenna structure for UHF RFID tags," International Journal of Microwave and Wireless Technologies, vol. 9, pp.1419–1426, July 2017.

[12] Kenari, M. A., M. N. Moghadasi, R. A. Sadeghzadeh, B. S. Virdee, and E. Limiti, "Dual-band RFID tag antenna based on the Hilbert-curve fractal for HF and UHF applications," IET Circuits, Devices & Systems, vol. 10, pp.140–146, 2016.

[13] Marindra, M. J., P. Pongpaibool, W. Wallada, and S. Siwamogsatham, "An optimized ink-reducing hollowed-out arm meander dipole antenna structure for printed RFID tags," International Journal of Microwave and Wireless Technologies, vol. 9, pp.469–479, March 2017.

[14] Barman B., S. Bhaskar, and A. K. Singh, "Spiral resonator loaded S-shaped folded dipole dual band UHF RFID tag antenna," Microwave and Optical Technology Letters, pp.1–7, 2018.

[15] Yang, P. H., Y. Li, L. Jiang, W. C. Chew, and T. T. Ye, "Compact metallic RFID tag antennas with a loop-fed method," IEEE Transactions on Antennas and Propagation, vol. 59, pp.4454–4462, December 2011.

[16] S.-Y. Kim, S.-H. Ahn, and W.-S. Lee, "Near-field UHF quadruple loop antenna with uniform field distribution for item-level tagging," IEEE Antennas and Wireless Propagation Letters, vol. 20, no. 4, April 2021, pp.523-527.

[17] D. Le, S. Ahmed, L. Ukkonen, and T. Björninen, "A small all- corners-truncated circularly polarized microstrip patch antenna on textile substrate for wearable passive UHF RFID tags," IEEE Journal of Radio Frequency Identification, vol. 5, no. 2, June 2021, pp.106-112.

[18] D. Dobrykh, I. Yusupov, S. Krasikov, A. Mikhailovskaya, D. Shakirova, A. A. Bogdanov, A. Slobozhanyuk, D. Filonov, and P. Ginzburg, "Long-range miniaturized ceramic RFID tags," IEEE Transactions on Antennas and Propagation, vol. 69, no. 6, June 2021, pp.3125-3131.

[19] M.-T. Nguyen, Y.-F. Lin, C.-H. Chen, C.-H. Chang, and H.-M. Chen, "Shorted patch antenna with multi slots for a UHF RFID tag attached to a metallic object," IEEE Access, vol.9, 2021, pp.111277-111292.

[20] S. Bhaskar and A.K. Singh, "A Compact meander line UHF RFID antenna for passive tag applications," Progress in Electromagnetics Research M, vol. 99, pp. 57-67, 2021.

[21] https://www.gs1.org/docs/epc/uhfg2_1_1_0-TestMethod-TagParameters_1_1_3-20080630.pdf

[22] J. Tan and X. Li, "Wideband double-UT RFID tag antenna design," Proc. Asia Pacific Conf. IEEE Circuits Syst., pp. 1256–1259, 2008.

[23] C. Cho, H. Choo, and I. Park, “Broadband RFID tag antenna with quasi-isotropic radiation pattern,” Electron. Lett. vol. 41, pp. 1091–1092, 2005.
[24] L. Mo, H. Zhang, and H. Zhou, “Broadband UHF RFID tag antenna with a pair of U slots mountable on metallic objects,” Electron. Lett., vol. 44, pp. 1173–1174, 2008.
[25] J. Z. Huang, P. H. Yang, W. C. Chew, and T. T. Ye, “A compact broadband patch antenna for UHF RFID tags,” Proc. Asia Pacific Conf. Microw., 2009, pp. 1044–1047.
[26] L. Xu, B. J. Hu, and J. Wang, “UHF RFID tag antenna with broadband characteristic,” Electron. Lett., vol. 44, pp. 79–80, 2008.
[27] A. G. Santiago, J. R. Costa, and C. A. Fernandes, “Broadband UHF RFID passive tag antenna for near-body applications,” IEEE Antennas Wireless Propag. Lett., vol. 12, pp. 136–139, 2013.
[28] J. Zhang and Y. Long, “A dual-layer broadband compact UHF RFID tag antenna for platform tolerant application,” IEEE Trans. Antennas Propag., vol. 61, no. 9, pp. 4447–4455, Sep. 2013.
[29] A. E. Hamraoui, E. H. Abdelmounim, J. Zbitou, H. Bennis, M. Latrach, and A. Errkik, “A low cost miniature UHF RFID tag antenna using paper substrate,” Proc. Int. Conf. Wireless Technol., Embedded Intell. Syst., 2017, pp. 1–6.
[30] F.-L. Bong, E.-H. Lim, and F.-L. Lo, “Miniaturized dipolar patch antenna with narrow meandered slotline for UHF tag,” IEEE Trans. Antennas Propag., vol. 65, pp. 4435–4442, 2017.
[31] F.-L. Bong, E.-H. Lim, and F.-L. Lo, ‘‘Compact orientation insensitive dipolar patch for metal-mountable UHF RFID tag design,’’ IEEE Trans. Antennas Propag., vol. 66, no. 4, pp. 1788–1795, Apr. 2018